Inorganic Chemistry
Article

Inorg. Chem. **2009**, *48*, 10389–10396 **10389**
DOI: 10.1021/ic901702s

Oxidation of Cyclohexane by High-Valent Iron Bispidine Complexes: Tetradentate versus Pentadentate Ligands

Peter Comba,* Martin Maurer, and Prabha Vadivelu

Universität Heidelberg, Anorganisch-Chemisches Institut, INF 270, D-69120 Heidelberg, Germany

Received August 27, 2009

The iron-bispidine-catalyzed oxidation of cyclohexane with H_2O_2, where either a tetradentate or a pentadentate bispidine ligand is coordinated to the iron center, yields up to 35% cyclohexanol and cyclohexanone (alcohol/ketone ratio of up to 4). Product distribution (including ^{18}O labeling studies), kinetic isotope effects, and the ratio of tertiary/secondary alcohols with adamantane as a substrate (3°/2°) suggest that (i) H abstraction by a ferryl complex is the rate-determining step and that the emerging cyclohexyl radical is short-lived, (ii) there is a parallel reaction involving oxidation by OH radicals, and (iii) there are considerable differences in the reaction pathways between the tetradentate and pentadentate ligand catalyst. These interpretations are fully supported by a DFT-based computational analysis.

Introduction

High-valent nonheme iron model complexes are of interest due to their relevance as biomimetic systems and their efficiency and selectivity in the catalytic oxidation of C−H and C=C bonds.[1−4] In the past decade, the first nonheme oxoiron(IV) intermediates in structurally characterized enzymes were trapped and spectroscopically characterized, and detailed mechanistic studies of nonheme oxygenases and halogenases were reported.[5−9] In parallel, the first well-characterized high-valent nonheme iron model systems were published, with detailed spectroscopic characterization and the first crystal structural analyses appearing.[10−12] An interesting feature is that natural systems generally have high-spin ($S = 2$) Fe^{IV}=O active sites,[5−8] while the biomimetic systems generally have intermediate-spin ($S = 1$) ferryl centers, with the exception of the aqua ion,[13] a recently reported pentacoordinate system,[14] and some of the bispidine systems reported here,[15] although full experimental proof is still missing in the latter systems.

There is some ambiguity with respect to the catalytically active oxidant, and Fe^{III}−OOH, as in activated bleomycine,[16−18] its decay products Fe^{V}=O (heterolytic O−O cleavage)[19,20] and Fe^{IV}=O together with OH radicals (homolytic cleavage),[21−25] as well as the products of direct

*To whom correspondence should be addressed. Fax: +49-6226-546617. E-mail: peter.comba@aci.uni-heidelberg.de.

(1) Meunier, B. *Biomimetic Oxidations Catalyzed by Transition Metal Complexes*; Imperial College Press: London, 2000.
(2) Chen, K.; Costas, M.; Que, L., Jr. *J. Chem. Soc., Dalton Trans.* **2002**, 672.
(3) Costas, M.; Mehn, M. P.; Jensen, M. P.; Que, L., Jr. *Chem. Rev.* **2004**, *104*, 939.
(4) Chen, M. S.; White, M. C. *Science* **2007**, *318*, 713.
(5) Price, J. C.; Barr, E. W.; Tirupati, B.; Bollinger, J. M., Jr.; Krebs, C. *Biochemistry* **2003**, *42*, 7497.
(6) Price, J. C.; Barr, E. W.; Glass, T. E.; Krebs, C.; Bollinger, J. M., Jr. *J. Am. Chem. Soc.* **2003**, *125*, 13008.
(7) Proshlyakov, D. A.; Henshaw, T. F.; Monterosso, G. R.; Ryle, M. J.; Hausinger, R. P. *J. Am. Chem. Soc.* **2004**, *126*, 1022.
(8) Riggs-Gelasco, P. J.; Price, J. C.; Guyer, R. B.; Brehm, J. H.; Barr, E. W.; Bollinger, J. M., Jr.; Krebs, C. *J. Am. Chem. Soc.* **2004**, *126*, 8108.
(9) Blasiak, L. C.; Vaillancourt, F. H.; Walsh, C. T.; Drewman, C. L. *Nature* **2006**, *440*, 368.
(10) Grapperhaus, C. A.; Mienert, B.; Bill, E.; Weyhermüller, T.; Wieghardt, K. *Inorg. Chem.* **2000**, *39*, 5306.
(11) Rohde, J.-U.; In, J.-H.; Lim, M. H.; Brennessel, W. W.; Bukowski, M. R.; Stubna, A.; Münck, E.; Nam, W.; Que, L., Jr. *Science* **2003**, *299*, 1037.
(12) Lim, M. H.; Rohde, J.-U.; Stubna, A.; Bukowski, M. R.; Costas, M.; Ho, R. Y. N.; Münck, E.; Nam, W.; Que, L., Jr. *Proc. Natl. Acad. Sci., U. S. A.* **2003**, *100*, 3665.
(13) Pestovsky, O.; Stoian, S.; Bominaar, E. L.; Shan, X.; Münck, E.; Que, L., Jr.; Bakac, A. *Angew. Chem., Int. Ed.* **2005**, *44*, 6871.
(14) England, J.; Martinho, M.; Farquhar, E. R.; Frisch, J. R.; Bominaar, E. L.; Münck, E.; Que, L., Jr. *Angew. Chem., Int. Ed.* **2009**, *48*, 3622.
(15) Bautz, J.; Comba, P.; Lopez de Laorden, C.; Menzel, M.; Rajaraman, G. *Angew. Chem., Int. Ed.* **2007**, *46*, 8067.
(16) Burger, R. M.; Peisach, J.; Horwitz, S. B. *J. Biol. Chem.* **1981**, *256*, 11636.
(17) Sam, J. W.; Tang, X. J.; Peisach, J. *J. Am. Chem. Soc.* **1994**, *166*, 5250.
(18) Decker, A.; Chow, M. S.; Kemsley, J. N.; Lehnert, N.; Solomon, E. I. *J. Am. Chem. Soc.* **2006**, *128*(14), 4719.
(19) Burger, R. M. *Chem. Rev.* **1998**, *98*, 1153.
(20) Stubbe, J.; Kozarich, J. W.; Wu, W.; Vanderwall, D. E. *Acc. Chem. Res.* **1996**, *29*, 322.
(21) MacFaul, P. A.; Ingold, K. U.; Wayner, D. D. M.; Que, L., Jr. *J. Am. Chem. Soc.* **1997**, *119*, 10594.
(22) MacFaul, P. A.; Arends, I. W. C. E.; Ingold, K. U.; Wayner, D. D. M. *J. Chem. Soc. Perkin Trans. 2* **1997**, 135.
(23) Arends, I. W. C. E.; Ingold, K. U.; Wayner, D. D. M. *J. Am. Chem. Soc.* **1995**, *117*, 4710.
(24) Kaizer, J.; Costas, M.; Que, L., Jr. *Angew. Chem., Int. Ed.* **2003**, *42*, 3671.
(25) Bautz, J.; Comba, P.; Que, L., Jr. *Inorg. Chem.* **2006**, *45*, 7077.

Published on Web 10/08/2009

oxidation of Fe^{II} to Fe^{IV} [15,26,27] have been proposed. Some of the relevant suggestions are based on the spectroscopic characterization of the iron-based intermediates as well as on labeling studies and the thorough analysis of the transformed substrates. In the catalytic oxidation of alkanes (typically cyclohexane), it is believed that metal-based oxidants (either Fe^{IV}=O or Fe^{V}=O) predominantly yield the alcohols; that is, hydrogen abstraction by the ferryl oxidant leads to carbon-based radicals which are rebound to the Fe−OH species to produce the alcohol product. Oxidation of the substrate by OH radicals is suggested to lead to carbon-based radicals that are trapped by O_2 to generate equimolar amounts of alcohol and ketone.[19−23]

The catalytic oxidation of cyclohexane by [(N4py)Fe(NCMe)]$(ClO_4)_2$/H_2O_2 (N4py = N,N′-bis(2-pyridylmethyl)-N-bis(2-pyridyl)methylamine) was thoroughly investigated with a variety of mechanistic probes, leading to the initial proposal that an OH-radical-based process leads to long-lived alkyl radicals.[28] However, with radical traps, there was only partial quenching of the reactivity. That is, a more selective additional oxidant, that is, $[(N4py)Fe^{IV}{=}O]^{2+}$, was thought to be also involved, and this was later trapped and fully characterized.[29]

The rigid pentadentate bispidine derivatives (see L^2 and L^3 in Scheme 1) have donor sets similar to N4py, and the bispidine-iron complexes are among the most active oxidation catalysts in nonheme iron chemistry.[30,31] Similar to the N4py-based system, the high-spin Fe^{II} complexes of L^2 and L^3 yield a metastable purple intermediate upon reaction with H_2O_2 in MeOH at −40 °C, assigned spectroscopically to low-spin $[(L^{2,3})Fe^{III}(\eta^1\text{-OOH})]^{2+}$. The isomeric L^2- and L^3-based systems have strikingly different reactivities but follow basically identical reaction pathways, and this is also confirmed in DFT studies.[30,32] However, the corresponding L^1-based tetradentate bispidine complex has completely different characteristics: with one exception,[25] no Fe^{III} intermediates were trapped, suggesting a direct Fe^{II} to Fe^{IV} pathway upon oxidation with H_2O_2,[26,27] and the high-valent complexes were shown to be quite different compared to the $L^{2,3}$-based systems in terms of their structure, electronics, and reactivity.[15,33,34]

Here, we report a detailed combined experimental and density functional theory (DFT)-based theoretical study on the catalytic oxidation of cyclohexane with the $[Fe(L^2)(NCMe)]^{2+}$/H_2O_2 and $[Fe(L^3)(NCMe)]^{2+}$/H_2O_2 systems, in comparison to the previously reported $[Fe(L^1)(NCMe)_2]^{2+}$/H_2O_2 system.

Scheme 1. Molecular Structures of L^1, L^2, and L^3 and Their Iron Complexes (X Is a Solvent Molecule or the Oxo Group)

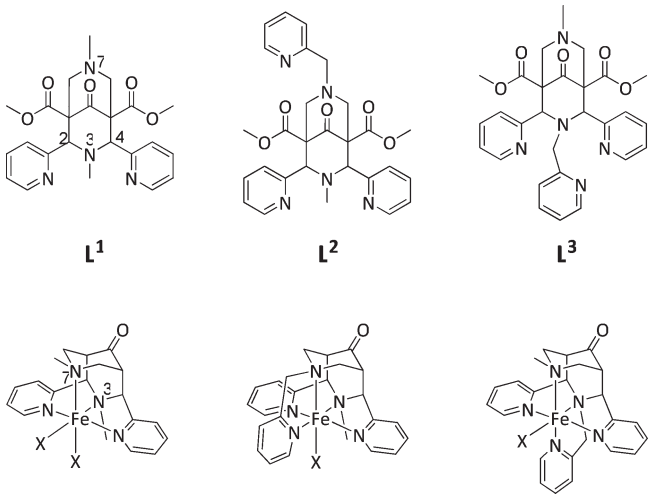

Experimental Section

Oxidation Experiments. The bispidine ligands and the corresponding iron(II) complexes were prepared as described before.[35] The standard reaction conditions for the catalytic oxidations are similar to those used before:[33] 0.3 mL of a H_2O_2 solution in MeCN (210 μmol, diluted from a 30% H_2O_2/H_2O solution) was delivered via syringe pump over 30 min at 25 °C to a stirring MeCN mixture (2.7 mL) containing the iron bispidine complex (2.1 μmol) and the substrate (2.1 mmol for cyclohexane, 0.21 mmol for adamantane). In the case of $[(L^1)Fe(NCMe)_2]^{2+}$ and $[(L^2)Fe(NCMe)]^{2+}$, the solutions were stirred for an extra 5 min after the H_2O_2 addition was completed; for $[(L^3)Fe(NCMe)]^{2+}$, there was an extra 270 min of stirring. In the experiments with acetone as the solvent, the conditions were as those used as with MeCN. To determine the kinetic isotope effects (KIE), substrate mixtures of cyclohexane and cyclohexane-d_{12} with 1:3 ratios were used. The products were filtered over a short silica gel plug and analyzed by GC (Varian GC 3900 with a ZB-1701 column); naphtalene was used as the internal standard.

In the case of the ^{18}O isotope labeling studies, 10 equiv of hydrogen peroxide (21 μmol) were added slowly via syringe pump. In experiments with $H_2{}^{18}O$, 38 μL of $H_2{}^{18}O$ (2.1 mmol) were added before the addition of H_2O_2. In experiments with $H_2{}^{18}O_2$, labeled hydrogen peroxide (2% H_2O_2/H_2O solution) was used. In reactions under $^{18}O_2$, the reaction mixture and the H_2O_2 solution were degassed three times before the reaction was started. The reactions were quenched by the addition of 0.1 mL of 1-methylimidazole, and the alcohol was transformed to an ester by the addition of acetic anhydride (1 mL). The ratio of the labeled and the unlabeled products was determined by GC-MS analysis: cyclohexanol (CI) m/z = 143 (^{16}O) and 145 (^{18}O).

Computational Details. All calculations were performed with DFT, using the Jaguar 6.5 program package[36] with the B3LYP functional[37−39] and the LACVP basis set (double ζ with a Los Alamos effective core potential for the Fe center, and 6-31G for the other atoms).[40] The intermediates were confirmed by frequency calculations (Gaussian 03[41]) as minima on the potential energy surface. To obtain reliable energetics, single-point

(26) Bautz, J.; Bukowski, M.; Kerscher, M.; Stubna, A.; Comba, P.; Lienke, A.; Münck, E.; Que, L., Jr. *Angew. Chem., Int. Ed.* **2006**, *45*, 5681.
(27) Comba, P.; Rajaraman, G.; Rohwer, H. *Inorg. Chem.* **2007**, *46*, 3826.
(28) Roelfes, G.; Lubben, M.; Hage, R.; Que, L., Jr.; Feringa, B. L. *Chem.—Eur. J.* **2000**, *6*, 2152.
(29) Klinker, E. J.; Kaizer, J.; Brennessel, W. W.; Woodrum, N. L.; Cramer, C. J.; Que, L., Jr. *Angew. Chem., Int. Ed.* **2005**, *44*, 3690.
(30) Bukowski, M. R.; Comba, P.; Limberg, C.; Merz, M.; Que, L., Jr.; Wistuba, T. *Angew. Chem., Int. Ed.* **2004**, *43*, 1283.
(31) Bukowski, M. R.; Comba, P.; Lienke, A.; Limberg, C.; Lopez de Laorden, C.; Mas-Balleste, R.; Merz, M.; Que, L., Jr. *Angew. Chem., Int. Ed.* **2006**, *45*, 3446.
(32) Comba, P.; Rajaraman, G. *Inorg. Chem.* **2008**, *47*, 78.
(33) Comba, P.; Maurer, M.; Vadivelu, P. *J. Phys. Chem. A* **2008**, *112*, 13028.
(34) Comba, P.; Kerscher, M.; Schiek, W. *Prog. Inorg. Chem.* **2007**, *55*, 613.
(35) Börzel, H.; Comba, P.; Hagen, K. S.; Merz, M.; Lampeka, Y. D.; Lienke, A.; Linti, G.; Pritzkow, H.; Tsymbal, L. V. *Inorg. Chim. Acta* **2002**, *337*, 407.
(36) *JAGUAR*, 6.5 ed.; Schrödinger LLC: New York, 2005.
(37) Becke, A. D. *J. Chem. Phys.* **1992**, *96*, 2155.
(38) Becke, A. D. *J. Chem. Phys.* **1992**, *97*, 9713.
(39) Becke, A. D. *J. Chem. Phys. B* **1993**, *98*, 5648.
(40) Hay, J. P.; Wadt, W. R. *J. Chem. Phys.* **1985**, *82*, 99.

calculations were performed on the B3LYP/LACVP-optimized geometries, using the LACV3P++** basis set (LanL2DZ for the Fe center and 6-311++G** for the remaining atoms). Solvation by MeCN was calculated at this level with single-point calculation using the polarized continuum model.[42−45] The quoted energies are those calculated at the B3LYP/LACV3P++** level and include entropy corrections (i.e., the reported energies are free energies), derived from the B3LYP/LACVP calculations and including solvent corrections.

Results and Discussion

Experimental Data. The iron-catalyzed oxidation of cyclohexane with H_2O_2 was performed under aerobic (O_2) and anaerobic (Ar) conditions at 25 °C. The experiments were done in MeCN as the solvent, and some were also done in acetone to trap emerging OH radicals. Generally, 100 equiv of H_2O_2 [i.e., the maximum turnover number (TON) is 100] was added slowly via syringe pump to a mixture of the iron catalyst and substrate; the samples for GC analysis were taken after 5 additional minutes of stirring for $[(L^1)Fe^{II}(NCMe)_2]^{2+}$ and $[(L^2)Fe^{II}(NCMe)]^{2+}$. With $[(L^3)Fe^{II}(NCMe)]^{2+}$, the reaction was much slower, and the mixture was stirred for an extra 270 min. Most of the results of the catalyst with the tetradentate ligand L^1 were reported previously,[33] and these are assembled in Table 1 together with the data emerging from the other two catalyst systems studied for this report.

Previous experiments indicated that the $[(L^1)Fe^{II}(NCMe)_2]^{2+}$ precatalyst, oxidized with peroxides or oxo-transfer agents to the corresponding ferryl complex, is a reasonably active oxidation catalyst (Table 1, entry 1),[33] and the corresponding data for the L^2- and L^3-based reactions suggest that these systems have a little lesser but similar activities (Table 1, entries 5 and 9). For a more complete mechanistic analysis, the KIE (reactions with mixtures of cyclohexane and cyclohexane-d_{12}) and the preference for tertiary over secondary alcohol formation with adamantane (3°/2°; stabilization of the tertiary radical intermediate) were also determined (see Table 1; high values for KIE and 3°/2° are a qualitative indication for hydrogen abstraction being the rate-determining step and for a significant lifetime of the radical intermediate).

Table 1. Catalytic Oxidation of Cyclohexane Catalyzed by $[(L^1)Fe^{II}(NCMe)_2]^{2+}$, $[(L^2)Fe^{II}(NCMe)]^{2+}$, or $[(L^3)Fe^{II}(NCMe)]^{2+}$

entry	ligand	experimental conditions	alcohol[a]	ketone[a]	A/K	KIE[b]	3°/2°[c]
1	L^1	MeCN, Ar	20.5(11)	13.5(5)	1.5	5.2(1)	17.0(9)
2	L^1	MeCN, O_2	13.2(2)	11.6(6)	1.1		27.5(7)
3	L^1	acetone, Ar	8.5(2)	8.8(1)	1.0		
4	L^1	acetone, O_2	8.0(6)	11.8(8)	0.7		
5	L^2	MeCN, Ar	16.5(15)	7.7(5)	2.1	2.2(1)	3.6(3)
6	L^2	MeCN, O_2	12.1(3)	10.8(1)	1.1		3.6(1)
7	L^2	acetone, Ar	15.6(6)	3.9(1)	4.0		
8	L^2	acetone, O_2	11.2(4)	10.6(2)	1.1		
9	L^3	MeCN, Ar	9.8(12)	9.9(11)	1.0	3.8(1)	5.0(2)
10	L^3	MeCN, O_2	8.9(2)	11.6(2)	0.8		4.5(1)
11	L^3	acetone, Ar	11.3(8)	6.0(4)	1.9		
12	L^3	acetone, O_2	12.8(2)	13.0(6)	1.0		

[a] Turnover number (TON) = moles of product per moles of catalyst; std in parentheses. [b] Kinetic isotope effect (KIE); mixture of cyclohexane and cyclohexane-d_{12} as substrate; std in parentheses. [c] 3°/2° = 3 × [3°-ol/(2°-ol + 2°-one)] with adamantane as substrate; std in parentheses.

The data for the L^1-based catalyst system indicate that the iron-catalyzed reaction is far more selective in the activation of C−H bonds than one would expect from hydroxyl radicals: a KIE of 5.2 and a 3°/2° of 17 in anaerobic and 27.5 in aerobic conditions, see entries 1 and 2 in Table 1, are much larger than those observed for hydroxyl-radical-based processes[46,47] and similar to those reported for heme iron systems, where the ferryl units are known to abstract hydrogen atoms.[48−50] The interpretation that $[(L^1)Fe^{IV}{=}O]^{2+}$ is responsible for the hydrogen atom abstraction, leading to a cyclohexyl radical of significant lifetime, was also supported by a DFT-based theoretical analysis.[33]

With 24% and 20% yield for the L^2- and L^3-based systems (entries 5 and 9 in Table 1), these are found to be reasonably good oxidation catalysts and similar to each other. However, $[Fe(L^3)(NCMe)](OTf)_2$ reacts much slower (300 min to completion of the reaction) than $[Fe(L^2)(NCMe)](OTf)_2$ (35 min). The L^2-based system has an A/K ratio (mol alcohol/mol ketone) of 2.1 under Ar and 1.0 with nearly identical overall yield in the presence of O_2 (Table 1, entries 5 and 6). This is a similar behavior to that of the tetradentate ligand L^1-based catalyst and suggests that O_2 might trap some of the cyclohexyl radicals. The resulting peroxo radicals might then react in a Russell-type mechanism to yield equimolar amounts of alcohol and ketone (see Scheme 2).[51] The reaction with the L^3-based catalyst leads to an A/K ratio of 1.0 under anaerobic conditions and to a slight excess of ketone in air (Table 1, entries 9 and 10). The KIE values of the two pentadentate ligand catalysts are smaller than that of the tetradentate bispidine catalyst (2.2 for L^2, 3.8 for L^3, 5.2 for L^1), suggesting that OH radicals might be involved in the cyclohexane oxidation (k_H/k_D between 1.0 and 2.0[46,47]). This is supported by the 3°/2° ratios in the

(41) Frisch, M. J.; Trucks, G. W.; Schlegel, H. B.; Scuseria, G. E.; Robb, M. A.; Cheeseman, J. R.; Montgomery, J. A., Jr.; Vreven, T.; Kudin, K. N.; Burant, J. C.; Millam, J. M.; Iyengar, S. S.; Tomasi, J.; Barone, V.; Mennucci, B.; Cossi, M.; Scalmani, G.; Rega, N.; Petersson, G. A.; Nakatsuji, H.; Hada, M.; Ehara, M.; Toyota, K.; Fukuda, R.; Hasegawa, J.; Ishida, M.; Nakajima, T.; Honda, Y.; Kitao, O.; Nakai, H.; Klene, M.; Li, X.; Knox, J. E.; Hratchian, H. P.; Cross, J. B.; Bakken, V.; Adamo, C.; Jaramillo, J.; Gomperts, R.; Stratmann, R. E.; Yazyev, O.; Austin, A.; Cammi, R.; Pomelli, C.; Ochterski, J. W.; Ayala, P. Y.; Morokuma, K.; Voth, G. A.; Salvador, P.; Dannenberg, J. J.; Zakrzewski, V. G.; Dapprich, S.; Daniels, A. D.; Strain, M. C.; Farkas, O.; Malick, D. K.; Rabuck, A. D.; Raghavachari, K.; Foresman, J. B.; Ortiz, J. V.; Cui, Q.; Baboul, A. G.; Clifford, S.; Cioslowski, J.; Stefanov, B. B.; Liu, G.; Liashenko, A.; Piskorz, P.; Komaromi, I.; Martin, R. L.; Fox, D. J.; Keith, T.; Al-Laham, M. A.; Peng, C. Y.; Nanayakkara, A.; Challacombe, M.; Gill, P. M. W.; Johnson, B.; Chen, W.; Wong, M. W.; Gonzalez, C.; Pople, J. A. *Gaussian 03*; Gaussian Inc.: Wallingford, CT, 2003.
(42) Cancès, M. T.; Mennucci, B.; Tomasi, J. *J. Chem. Phys.* **1997**, *107*, 3032.
(43) Cossi, M.; Barone, B.; Mennucci, B.; Tomasi, J. *Chem. Phys. Lett.* **1998**, *286*, 253.
(44) Mennucci, B.; Tomasi, J. *J. Chem. Phys.* **1997**, *106*, 5151.
(45) Cossi, M.; Scalmani, G.; Raga, N.; Barone, V. *J. Chem. Phys.* **2002**, *117*, 43.
(46) Buxton, G. V.; Greenstock, C. L.; Helman, W. P.; Ross, A. B. *J. Phys. Chem. Ref. Data* **1988**, 513.
(47) Sawyer, D. T.; Kang, C.; Llobet, A.; Redman, C. *J. Am. Chem. Soc.* **1993**, *115*, 5817.
(48) Sono, M.; Roach, M. P.; Coulter, E. D.; Dawson, J. H. *Chem. Rev.* **1996**, *96*, 2841.
(49) Nesheim, J. C.; Lipscomb, J. D. *Biochemistry* **1996**, *10*, 240.
(50) Groves, J. T.; Nemo, T. E. *J. Am. Chem. Soc.* **1983**, *105*, 6243.
(51) Russell, G. A. *J. Am. Chem. Soc.* **1957**, *79*, 3871.

Scheme 2. Anaerobic (A) and Aerobic (B) Pathway for the Ferryl-Based Oxidation of Cyclohexane

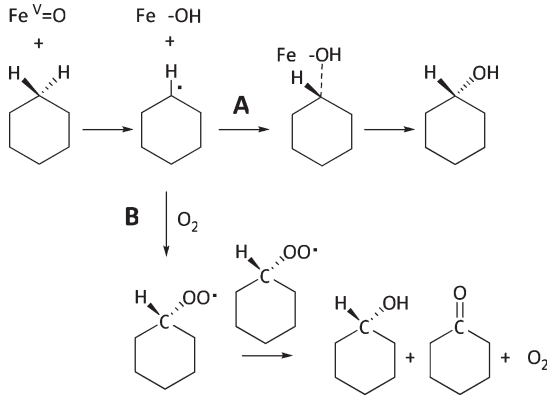

reaction with adamantane, which decrease from 17 for L^1 to 3.6 and 5.0 for the pentadentate ligand systems.

In acetone as a hydroxyl radical trap, the yield of the oxidation of cyclohexane with the L^1-based catalyst is decreased by nearly 50% with identical amounts of alcohol and ketone (entry 3 in Table 1).[52] With the L^2-based catalyst, there is a small decrease of the overall yield and a shift of the A/K ratio with increasing alcohol selectivity (Table 1, entry 7); with the L^3-based system, there is a similar trend (Table 1, entry 11). In the presence of O_2, the A/K ratio decreases with both pentadentate ligands, as one would expect when the alkyl radicals are trapped by O_2 (see Scheme 2; entries 8 and 12 in Table 2). The conclusions from the data in Table 1 are that (i) OH radicals are involved in the oxidation of cyclohexane and (ii) there must be another oxidant when OH radicals are trapped, and this probably is a high-valent iron-oxo species.

^{18}O labeling experiments were all done in MeCN (see Table 2). With $[(L^1)Fe^{II}(NCMe)_2]^{2+}$ as the precatalyst, under Ar, there is around 10% ^{18}O incorporation into the alcohol product via H_2O; the rest is from H_2O_2. This is typical for Fe^{IV}=O-catalyzed reactions, and the 10% label from H_2O arises from H_2O exchange of the ferryl species.[53] With the L^2- and L^3-based catalysts, the results are similar and suggest some differences in the water exchange rates. The situation is drastically different in an aerobic atmosphere. While, with the tetradentate bispidine catalyst, there is around 60% of the alcohol oxygen atom arising from O_2 and 40% from H_2O_2, for both pentadentate bispidines, 100% of the oxygen atoms originate from O_2. It is interesting to remember here that, from the data in Table 1, we concluded that, for all three catalysts, a high-valent iron species is involved in the alcohol formation, and that the KIEs are related to hydrogen atom abstraction from the substrate. The drastically different KIE and 3°/2° values for the tetra- and pentadentate ligand catalysts might be related to the lifetime of the radical intermediate and to the relative rates of pathways A and B in Scheme 2 (relative energies

(52) Note that the results of the experiments in acetone should not be overinterpreted because the change of solvent may lead to a range of additional changes, including a variation of the redox potentials and a change of the spin ground state.

(53) Seo, M. S.; In, J.-H.; Kim, S. O.; Oh, N. Y.; Hong, J.; Kim, J.; Que, L.; Nam, W. *Angew. Chem., Int. Ed.* **2004**, *43*, 2417.

Table 2. Incorporation of ^{18}O into the Alcohol Product of the $[(L^1)Fe^{II}(NCMe)_2]^{2+}$-, $[(L^2)Fe^{II}(NCMe)]^{2+}$-, and $[(L^3)Fe^{II}(NCMe)]^{2+}$-Catalyzed Oxidation Reactions of Cyclohexane in MeCN

	^{18}O- labeled cyclohexanol product[a]				
	reaction under Ar		reaction under O_2		
ligand	$H_2{}^{18}O_2$	$H_2{}^{18}O$	O_2	$H_2{}^{18}O_2$	$H_2{}^{18}O$
L^1	87	7	59	40	
L^2	70	25	100		
L^3	95	6	100		

[a] Values in percent, determined from the relative height of the MS peaks of the labeled and unlabeled alcohol products.

of the three transition states involved). This could also account for the drastically different labeling data in aerobic conditions. Note, however, that this is not unambiguous, and the reoxidation of the iron catalyst by H_2O_2 or O_2 might also follow different pathways for the tetra- and pentadentate ligand systems, thus influencing the labeling data.

On the basis of the experimental data, we draw the following conclusions. (i) The pathways for the $[(L^1)Fe^{II}(NCMe)_2]^{2+}$-based catalyst is different from that for the $[(L^2)Fe^{II}(NCMe)]^{2+}$- and $[(L^3)Fe^{II}(NCMe)]^{2+}$-based systems. Specifically, the KIE and 3°/2° values are drastically different and suggest that there are significant differences with respect to the catalytically active species involved. (ii) The $[(L^2)Fe^{II}(NCMe)]^{2+}$ and $[(L^3)Fe^{II}(NCMe)]^{2+}$ precatalysts basically lead to identical yields and product distributions, but the L^3-based reaction is about 10-fold slower. A similar observation was made in the $[(L^2)Fe^{II}(NCMe)]^{2+}$- and $[(L^3)Fe^{II}(NCMe)]^{2+}$-catalyzed alkene oxidation with H_2O_2 (epoxidation and dihydroxylation),[31,32] and this supports the interpretation that the corresponding ferryl species rather than hydroxyl radicals are primarily responsible for the C−H activation. (iii) For $[(L^1)Fe^{II}(NCMe)_2]^{2+}$, the results suggested that both Fe^{IV}=O and Fe^{V}=O pathways might be involved.[33] For the pentadentate ligand systems, this does not seem to be a likely scenario. However, most of these interpretations are not unambiguous, and DFT was therefore used to help to solve some of the ambiguities.

DFT Calculations. The usual pathway for the oxidation of alkanes by high-valent iron complexes, supported in our system by the experimental data discussed above, involves an electrophilic attack of the C−H bond by the ferryl group (ts1), leading to the formation of Fe^{III}−OH and a radical intermediate (rad_{int}), which reacts over the rebound transition state (ts2) to the alcohol product coordinated to the Fe^{II} precatalyst (see Scheme 3). Important points of interest addressed in this computational part are the activation energy of the critical hydrogen abstraction step (reactivity of the catalyst), the lifetime of the radical intermediate, and the main differences of the reaction profiles between the pentadentate and tetradentate ligand systems. For the two catalysts with the pentadentate ligands L^2 and L^3, the $S = 1$ and $S = 2$ spin states were considered; the $S = 0$ state is destabilized by 127 kJ/mol and therefore not considered here.[32] Interestingly, the pentadendate ligand-based catalysts have an $S = 1$ ground state,[26] while in the tetradentate L^1-based

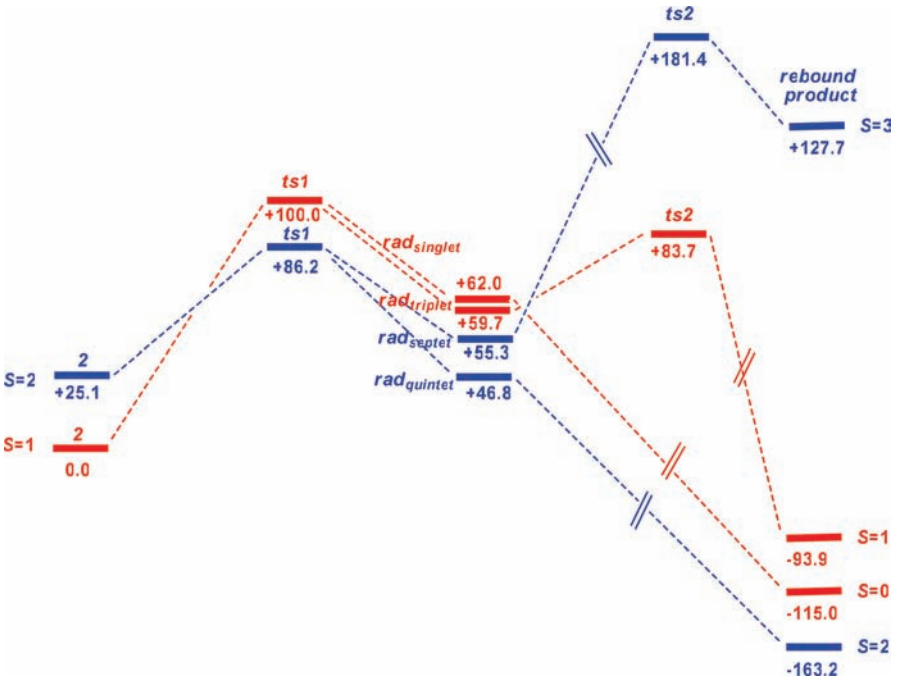

Figure 1. Computed free energy profile (kJ/mol) for the metal-based pathway of the $[(L^2)Fe^{IV}{=}O]^{2+}$-catalyzed cyclohexane hydroxylation.

Scheme 3. Mechanism of Cyclohexane Hydroxylation via a Metal-Based Oxidant (for clarity the H atoms are represented as small sticks)

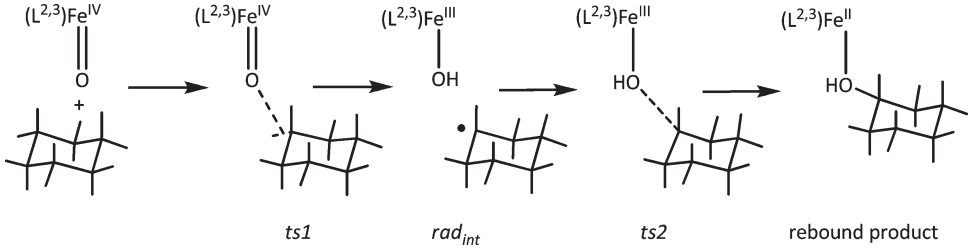

system with H_2O as the sixth ligand, the $S = 2$ spin state is believed to be the ground state.[15,33,54] However, all possible pathways were studied in analogy with the published work with the L^1-based ligand system.[33]

The two catalysts $[(L^2)Fe^{IV}{=}O]^{2+}$ and $[(L^3)Fe^{IV}{=}O]^{2+}$ are isomers which differ by the position of the oxo group (O is trans to N7 in the L^2-based and trans to N3 in the L^3-based catalyst, see Scheme 1). It is well-known that the L^3-based ferryl complex is more stable than the corresponding L^2-based isomer, and therefore, the latter is the stronger oxidant and more reactive catalyst.[30−32,55] The computed energy diagram for the oxidation of cyclohexane to cyclohexanol with the more reactive catalyst $[(L^2)Fe^{IV}{=}O]^{2+}$ is shown in Figure 1, and the optimized structures of the transition states are presented in Figure 2. The ferryl complex has an $S = 1$ ground state with the $S = 2$ spin state at +25.1 kJ/mol.[55] For the hydrogen transfer step, $\Delta G^{\ddagger}$ on the $S = 2$ spin surface is, as expected, lower (by 13.8 kJ/mol) than the $S = 1$ energy barrier. Magnetic coupling of the carbon-based radical with the Fe^{III} center in the emerging rad_{int} species leads to four possible electronic states with similar structures and energies (see Figure 1). It appears that rad_{int} on the $S = 2$ spin surface is slightly more stable. However, the more important question is the lifetime of the radical intermediate, and this depends on the relative energy of the rebound transition state (ts2). Unfortunately, we were not able to optimize this structure in all spin states. From the ferromagnetically coupled structures on the high- and low-spin surfaces, there are relatively large computed barriers of 126.1 and 24.0 kJ/mol, respectively. The exceedingly high barrier starting from the rad_{septet} radical ($\Delta G^{\ddagger}$ = +181.4 kJ/mol) is not unexpected due to the instability of the rebound product in an $S = 3$ configuration (+127.7 kJ/mol).[56,57] The computed profile from a stepwise variation of the distance between the radical carbon atom and the $Fe^{III}-O$ group of the $rad_{quintet}$ intermediate (relaxed PES scan) does not show any maximum. Also, when the ts2 structure derived from the $rad_{triplet}$ intermediate is used as a starting structure to predict the approximate energy of ts2 derived from $rad_{quintet}$ (the distance of the forming C−O bond was frozen to the value of the optimized ts2 structure derived from $rad_{triplet}$), the resulting approximate energy barrier is very small (2.3 kJ/mol). It therefore appears that

(54) Comba, P.; Wunderlich, S. *Chem.—Eur. J.* Submitted 2009.
(55) Anastasi, A.; Comba, P.; McGrady, J.; Lienke, A.; Rohwer, H. *Inorg. Chem.* **2007**, *46*, 6420.
(56) De Visser, S. P. *J. Am. Chem. Soc.* **2006**, *128*, 9813.
(57) De Visser, S. P. *J. Am. Chem. Soc.* **2006**, *128*, 15809.

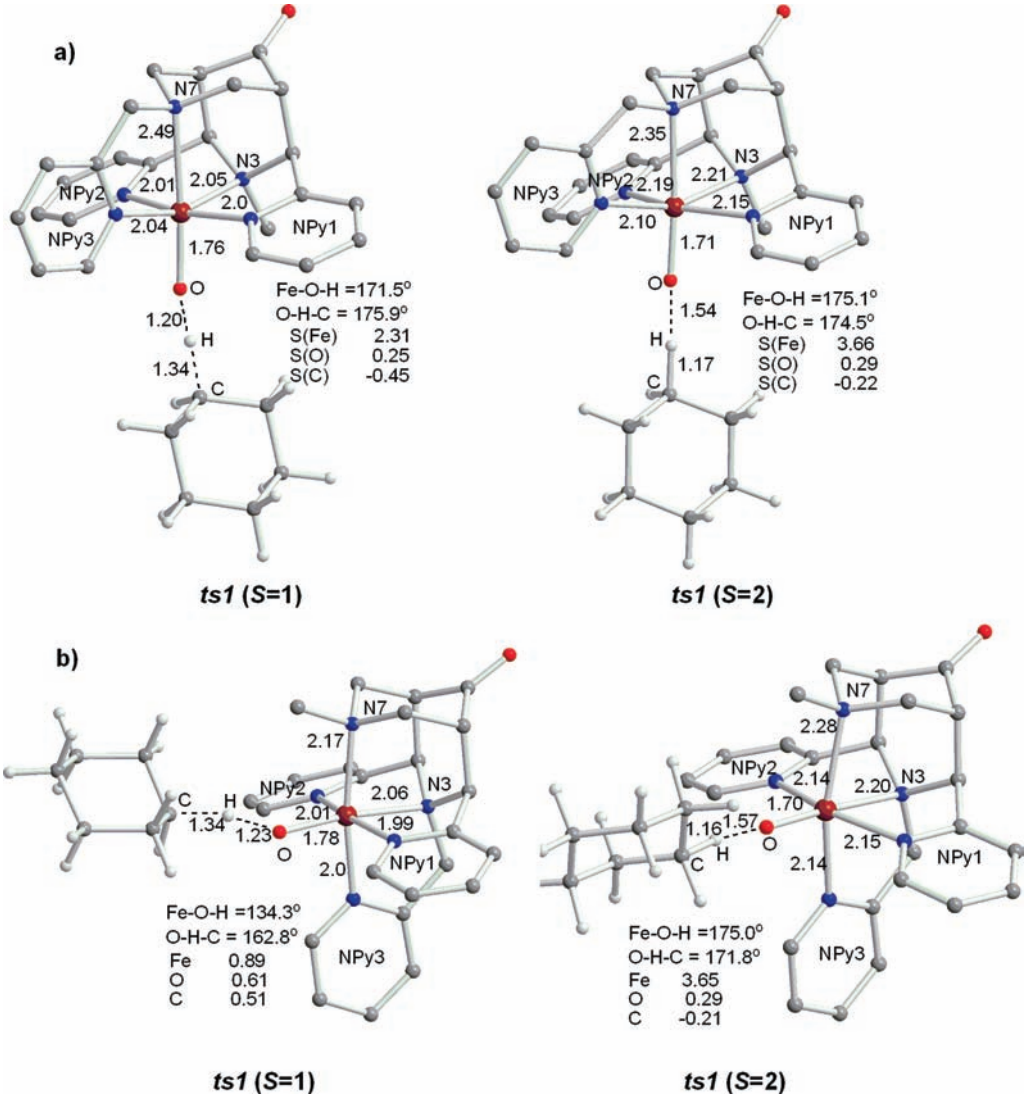

Figure 2. Computed geometries of (a) ts1 with $[(L^2)Fe^{IV}{=}O]^{2+}$ and (b) ts1 with $[(L^3)Fe^{IV}{=}O]$ as the catalyst for the $S = 1$ and $S = 2$ spin surfaces. Bond lengths in ångströms; valence angles in degrees.

Scheme 4. Formation of Short-Lived and Long-Lived Radicals Based on Different Types of Oxidants (the conversation of the short-lived to the long-lived rad_{int} corresponds to pathway B in Scheme 2, i.e., diffusion of the cyclohexyl radical away from the Fe−OH species; for clarity, the H atoms are represented as small sticks)

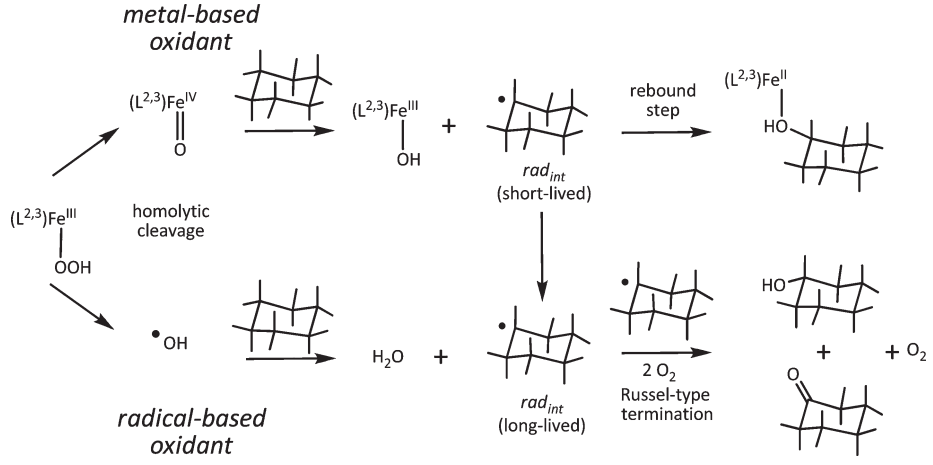

formation of the rebound product on the most favorable spin surface must be a process with a very low energy barrier; that is, the radical intermediate is very short-lived. This is in contradiction to the experimental observation of 100% incorporation of ^{18}O from $^{18}O_2$, suggesting that O_2 is captured by a long-lived intermediate. It follows that

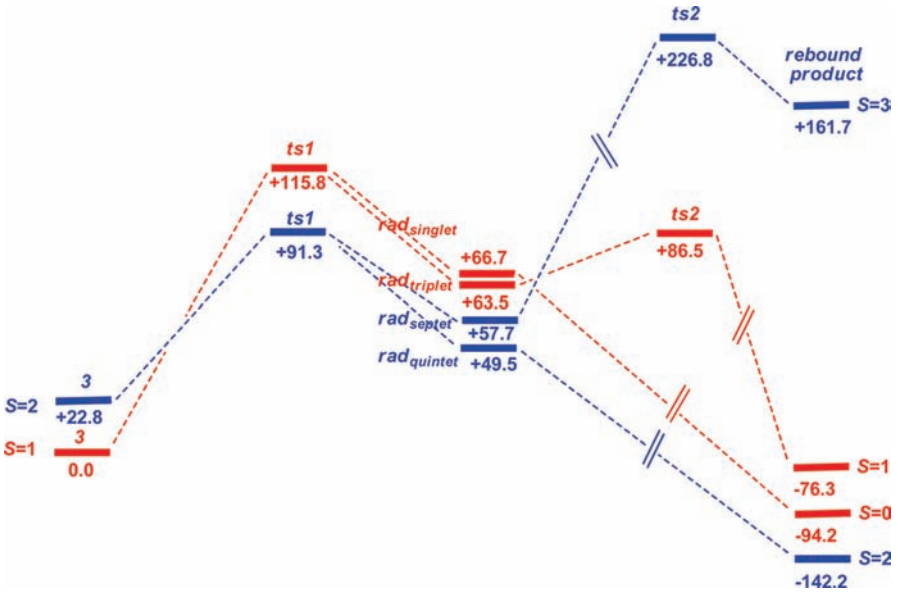

Figure 3. Computed free energy profile (kJ/mol) for the metal-based pathway of the $[(L^3)Fe^{IV}{=}O]^{2+}$-catalyzed cyclohexane hydroxylation.

there are probably two independent pathways to carbon-based radical intermediates (see Scheme 4), and that formed by OH radicals is expected to be longer-lived,[51] captures $^{18}O_2$, and decays in a Russel-type termination to equal amounts of cyclohexanol and cyclohexanone.[59]

The DFT-predicted properties of the less reactive $[(L^3)Fe^{IV}{=}O]^{2+}$ isomer (O is trans to N3) are very similar and are shown in the computed free energy profile in Figure 3 and the corresponding optimized transition state structures in Figure 2. In analogy to the L^2-based system, that of L^3 also has the $S = 1$ spin state as the electronic ground state (stabilized by 22.8 kJ/mol), and the reaction is expected to change to the high-spin surface since ts1 is considerably more stable in the $S = 2$ spin state (stabilized by 24.5 kJ/mol). The emerging radical intermediate is most stable in the quintet state and expected to decay to the rebound product in a close to barrierless reaction. The computed kinetic and thermodynamic parameters of $[(L^2)Fe^{IV}{=}O]^{2+}$ and $[(L^3)Fe^{IV}{=}O]^{2+}$ are assembled in Table 3. The rate-determining hydrogen abstraction step of $[(L^2)Fe^{IV}{=}O]^{2+}$ is predicted to be faster than that with $[(L^3)Fe^{IV}{=}O]^{2+}$ as the active catalyst, and this is as observed experimentally. Moreover, the reaction with the more active catalyst leads, as expected, to the more stable product. With both catalysts, the reaction primarily occurs on the $S = 2$ spin surface. The lower energy barrier involving ts1 on the high-spin surface is in agreement with shorter C−H (1.17 vs 1.34 Å) and longer O−H distances (1.54 vs 1.20 Å), see Figure 2 for the L^2-based system.

In contrast to the tetradentate bispidine L^1-based system, experimentally, there is no indication for an $Fe^V{=}O$-based pathway. However, in analogy to $[(L^1)Fe^V{=}O]^{3+}$, we have also considered this possibility in our DFT study. As with the tetradentate ligand system,[33] the $S = 3/2$ configuration is found to be the ground state for the $[(L^{2,3})Fe^V{=}O]^{3+}$ species, and this is stabilized by 30−35 kJ/mol from the $S = 1/2$ spin state. The catalytic activity of the two $Fe^V{=}O$ complexes was examined, and the main results are assembled in Table 3 (see the Supporting Information for computed energy profiles and relevant structures; as in our earlier study[33] and other published work,[60] we have not been able to refine the radical intermediate).[61] Consistent with the Fe^{IV} pathway, the catalysis with $[(L^2)Fe^V{=}O]^{3+}$ (where O is trans to N7) is faster than that with $[(L^3)Fe^V{=}O]^{3+}$ (where O is trans to N3, see Table 3). Note that the putative $Fe^V{=}O$ oxidants are, as one would expect, more reactive than the $Fe^{IV}{=}O$ systems. However, the difference is significantly smaller for the pentadentate than for the tetradentate ligand complexes. More importantly, the oxidation of the iron(II) precatalysts to iron(V) is much more difficult than that to the corresponding iron(IV) systems. While, for the tetradentate bispidines, it has been shown that this is an unfavorable but basically possible reaction,[25,27] this has not been shown to be the case for the pentadentate bispidine ligands.

Table 3. Overall Activation and Reaction Energies (kJ/mol) of $[(L^{2,3})Fe^{IV}{=}O]^{2+}$ on the $S = 2$ and of $[(L^{2,3})Fe^V{=}O]^{3+}$ on the $S = 3/2$ Surface (energies are relative to the ground state of the respective ferryl complexes)

complex	$\Delta G^{\ddagger}$	ΔG_{re}
$[(L^2)Fe^{IV}{=}O]^{2+}$	+86.2	−163.2
$[(L^3)Fe^{IV}{=}O]^{2+}$	+91.3	−142.2
$[(L^2)Fe^{V}{=}O]^{3+}$	+20.7	−263.0
$[(L^3)Fe^{V}{=}O]^{3+}$	+68.0	−262.3

Conclusion

High-valent iron-bispidine complexes are very efficient oxidation catalysts which are capable of oxidizing nonactivated

(58) Neta, P.; Schuler, R. H. *J. Phys. Chem.* **1975**, *79*, 1.
(59) Note that this is a different interpretation from that given above on the basis of the experimental data, but it is in agreement with the experimental results. The abstraction of a hydrogen atom from the substrate by an OH radical is generally believed to be a very fast reaction.[32,46,58]
(60) Johansson, A. J.; Blomberg, M. R. A.; Siegbahn, E. M. *J. Phys. Chem. C* **2007**, *111*, 12397.
(61) There is formation of $Fe^{IV}{=}O$ and a radical cation (electron transfer), and this is a common problem.[55] Decay to the rebound product is barrierless.

alkane C−H bonds. The efficiencies and mechanistic pathways of the tetradentate (L^1)- and pentadentate ($L^{2,3}$)-based complexes are strikingly different. With both groups of ligands, there is more than one active pathway. While, for the tetradentate ligand system, there is some indication that an Fe^V=O-based oxidation might be involved, this is an unlikely scenario for the pentadentate ligands discussed here. However, the experimental data suggest that alkane oxidation by OH radicals might be involved in addition to the ferryl-based hydrogen abstraction process, and this is supported by the striking differences in ^{18}O labeling in an aerobic atmosphere. An important feature not discussed here in detail is that the tetradentate bispidine ferryl system is assumed to have an $S = 2$ ground state,[15,62] and this might contribute to the higher efficiency of the L^1-based system.

Acknowledgment. We are grateful for generous financial support by the German Science Foundation (DFG).

Supporting Information Available: Computed geometries of transition states and free energy profiles of the $[(L^{2,3})Fe^V{=}O]^{3+}$ reactions are given. This material is available free of charge via the Internet at http://pubs.acs.org.

(62) Fukuzumi, S.; Kotani, H.; Lee, Y.-M.; Nam, W. *J. Am. Chem. Soc.* **2008**, *130*, 15134.